Low-cost, robust, filtered spectrometer for absolute intensity measurements in the soft x-ray region

N. E. Lanier[a)]
Los Alamos National Laboratory, Los Alamos, New Mexico 87544

S. P. Gerhardt
Department of Electrical Engineering, University of Wisconsin–Madison, Madison, Wisconsin 53706

D. J. Den Hartog
Department of Physics, University of Wisconsin–Madison, Madison, Wisconsin 53706

(Presented on 22 June 2000)

We have developed a low-cost, robust, multifoil-filtered spectrometer to provide absolute measurements of low-Z impurity concentrations in the Madison Symmetric Torus reversed-field pinch. The spectrometer utilizes an array of six thin-film coated soft x-ray diodes. Each multilayered coating is specifically tailored to isolate the *K*-shell emission lines of H- and He-like oxygen, carbon, and aluminum. With calibrations obtained via a synchrotron source, absolute measurements of photon flux have been made. We address the technical aspects of this diagnostic and present impurity data from both standard and high-confinement plasma discharges. © *2001 American Institute of Physics.* [DOI: 10.1063/1.1322619]

I. INTRODUCTION

Multifoil filter spectrometers have long been an attractive low-cost alternative to more traditional spectrometers, especially in instances where the spectrum of interest is dominated by bright, well-separated emission lines. The idea of an array of filters with their absorption edges providing spectral separation is an old one, first presented by Ross[1] in 1928, and later expanded by Kirkpatrick.[2,3] More recently, multifoil spectrometers have been proven very successful in obtaining routine measurements of impurities in reversed-field pinch (RFP) (Ref. 4) plasmas.[5,6]

In this article, we present absolute measurements of plasma impurities using a newly designed multifoil spectrometer. This new spectrometer was developed on the Madison Symmetric Torus (MST) (Ref. 7) RFP and offers the following improvements over past versions.[5] The thin-film multilayer filters have been directly deposited onto the detector surface eliminating the need for fragile freestanding filters. Two additional channels have been added to enhance measurement accuracy by quantifying the high- and low-energy components of the spectrum. The composition of the multilayer filters have been completely redesigned to enhance the isolation of specific lines. Finally, these filtered detectors have been calibrated via synchrotron light source, thus allowing absolute fluxes to be obtained.

II. BACKGROUND

Quantitative measurement of *K*-shell transitions offers the most reliable way to extract impurity state densities. These transitions result from hydrogen-like (H-like) and helium-like (He-like) low-Z impurity charge states that are prevalent in the MST core. The low electron temperatures and densities of MST discharges are insufficient to maintain local thermodynamic equilibrium (LTE). Hence, with radiative processes dominating over collisional ones, the coronal model is employed.

The density of any given charge state is dictated by the balance between ionization, particle loss, and recombination. For typical MST parameters, ($n_e \sim 0.8$–$1.2 \times 10^{+13} \, \mathrm{cm}^{-3}$, $T_e \sim 200$–$500 \, \mathrm{eV}$, and $T_i \sim 100$–$300 \, \mathrm{eV}$), the dominant ionization process results from electron impact. A distinction of standard MST discharges is the large concentration of neutral hydrogen in the plasma core ($\sim 10^{+10} \, \mathrm{cm}^{-3}$), and as a result, radiative and dielectronic recombination effects are negligible when compared with those of charge exchange. Along with charge-exchange recombination, transport losses play an important role in reducing the densities of low-Z impurity states. With impurity confinement times of order charge-exchange recombination times ($\tau_{\mathrm{imp}} \sim 2$–$8 \, \mathrm{ms}$), direct losses of low-Z impurity states are of similar magnitude to those lost via recombination.

Charge-state excitation is also dominated by the electron-impact process. Moreover, for H- and He-like low-Z impurities, the excited-state lifetimes are so short that virtually all excitations are followed by a single radiative decay back to the ground state. This balance between excitation and emission is the hallmark of the coronal model and allows the emissivity of a transition from states $i-j$ to be described as

$$\epsilon_\gamma^{j-i} = n_e n_{\mathrm{imp}} \langle \sigma v \rangle_{\mathrm{excitation}}^{(i-j)}, \tag{1}$$

where n_{imp} and n_e are the impurity state and electron densities and $\langle \sigma v \rangle_{\mathrm{excitation}}^{(i-j)}$ is the excitation rate for the $i-j$ transition.

A principal advantage in monitoring the *K*-shell transitions of H- and He-like ions is that the electron excitation rates are well characterized. For a system with a Maxwellian

---

a)Electronic mail: nlanier@lanl.gov

1188

TABLE I. Composition of the six multilayer filters, principal absorption edge employed, and the primary region of interest.

Filter	Composition	Principal absorption edge	Principal band of interest
1	1.0 μm Al, 6.0 μm Mylar[a]	None	<12 Å
2	4500 Å Fe, 5000 Å Al	17.5 Å	18–19 Å
3	5000 Å Mn, 4000 Å Al	19.5 Å	20–23 Å
4	5000 Å V, 5000 Å Al	24.3 Å	25–35 Å
5	1 μm CaF, 2500 Å Ag 2000 Å Al	36.0 Å	37–43 Å
6	7.5 μm polyimide[a] 1000 Å Al	43.7 Å	>45 Å

[a]Mylar and polyimide are freestanding.

temperature distribution, these rates are reported by Mewe[8] and should be accurate to within 30%–50%. Therefore, by measuring electron density (n_e), temperature (T_e), and photon emission from a well-characterized transition (ϵ_γ^{i-j}), Eq. (1) can be used to extract the impurity-state density (n_{imp}).

III. DIAGNOSTIC DESIGN THEORY

It is believed that the region between 5 and 50 Å is dominated by line emission and the spectrum can be approximated by a collection of delta functions with differing amplitudes, each representing a narrow band of emission. The filters of the spectrometer are designed to isolate the bands outlined in Table I. If we make this assumption, then the current measured in each diode can be approximated as a linear combination of the products of band emission and filter transmission. In other words, the measured diode current is

$$I_k = \sum_{i=1}^{n} \eta(\lambda_i) T_k(\lambda_i) \epsilon_i(\lambda_i) \delta(\lambda - \lambda_i), \qquad (2)$$

where $T_k(\lambda)$ is the filter transmission of the kth diode, $\epsilon(\lambda)$ is the band emissivity at wavelength λ, and $\eta(\lambda)$ is the photon conversion efficiency. For these wavelengths, the diodes are virtually 100% efficient, meaning the number of electrons per photon of wavelength λ is

$$\eta(\text{electrons}) = 3417/\lambda(\text{Å}). \qquad (3)$$

The ultimate goal of the multifoil spectrometer is to obtain the emissivity [$\epsilon(\lambda)$]. A closer inspection of Eq. (2) shows that the diode current (I) is just a matrix and can be written as

$$I = TR, \qquad (4)$$

where we have defined $R = \eta(\lambda)\epsilon(\lambda)$. By inverting the filter transmission matrix (T), we can directly solve for R and extract ϵ as follows:

$$\epsilon(\lambda) = \frac{[T^{-1}(\lambda)I]}{\eta(\lambda)}. \qquad (5)$$
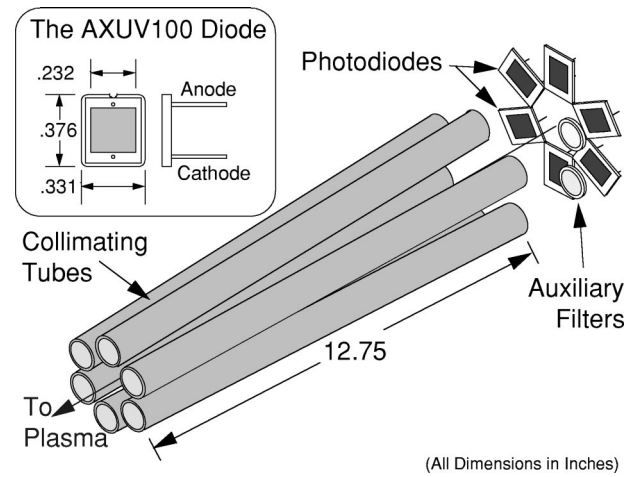

FIG. 1. Overview of the multifoil spectrometer layout. The inset displays the AXUV diode, the spectrometer's principal component.

With the simultaneous measurements from the six-diode array, the emission amplitudes of the six principal bands that dominate the spectrum can be extracted.

IV. DIAGNOSTIC

The multifoil spectrometer consists of six, tightly packed, soft x-ray photodiodes (Fig. 1). Collimators are used to control light levels and assure that each channel is viewing a similar chord through the plasma. Each diode is coated with an individual thin-film multilayer absorption filter, specifically designed to isolate a narrow band in the XUV region.

The multilayer filter characteristics are outlined in Fig. 2 and Table I. The principal concept in designing a thin-film multilayer filter is to properly choose materials that have natural absorption edges in the region of interest. To isolate the O VII ($\sim$ 18.6 Å for $1s^2 - 1s3p$, and $\sim$ 21.3 Å for $1s^2 - 1s2p$) and O VIII ($\sim$ 18.9 Å) emission, we use iron, manganese, and vanadium, which have absorption edges at 17.5, 19.5, and 24.3 Å, respectively. To separate the C V ($\sim$ 40 Å) and C VI ($\sim$ 33 Å) impurity states, the fluorine edge at 36 Å is used. The freestanding polyimide ($C_{22}H_{10}N_2O_5$) filter has a very strong carbon edge at $\sim$ 43.7 Å, which isolates C V from the lower-energy emissions of B IV. The first filter is designed to pass the high-energy com-
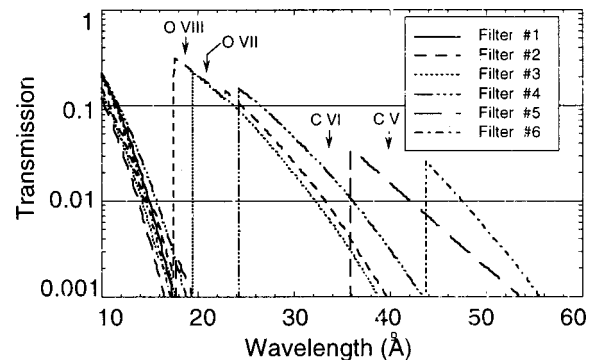
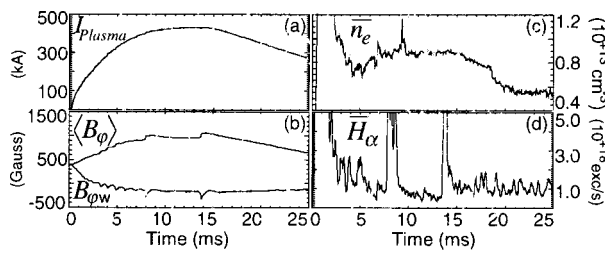

FIG. 2. Filter transmissions between 10 and 50 Å.

FIG. 3. (a) Plasma current, (b) average toroidal magnetic field and toroidal field measured at the wall, (c) line-averaged electron density measured through a central chord, and (d) the line-averaged H_α excitation rate (proportional to neutral particle density) for a typical high-current plasma discharge.

ponents ($\lambda < 15$ Å). Here, a freestanding Mylar ($C_{10}H_8O_4$) filter is used to attenuate wavelengths above 50 Å where the 1 μm aluminum becomes transparent.

The thin-film filters were designed using the XCAL (Ref. 9) software package. Measurements of their transmission properties were conducted at the National Synchrotron Light source at Brookhaven National Laboratory. The results of these measurements[10] indicate that the transmission characteristics were within the theoretical predictions obtained from XCAL.

The focal point of the six-channel diode array is the AXUV-100 (Ref. 11) silicon detector (inset in Fig. 1). The diode has an active area of 1 cm^2 and is virtually 100% efficient for photons above 10 eV. The large active area makes it ideal for situations where low-light levels are an issue. However, this comes at the expense of a large junction capacitance (C_j), which can dramatically reduce the time response of the detector. With the goal of measuring equilibrium impurity behavior, high speed was not required, and the system was designed to resolve fluctuations up to 40 kHz.

V. EXPERIMENTAL RESULTS

At its inception, the multifoil spectrometer was designed to enhance the robustness and emission-line isolation of its predecessor.[5] While the effectiveness of the new filters to isolate emissions from O VII and O VIII has surpassed expectation, measurements of C V and C VI are greatly hindered by the larger than expected nitrogen concentration. This rise in nitrogen concentration is attributed to recent diagnostic additions that have increased the amount of plasma-facing boron nitride, often employed as heat shielding. Moreover, the concentration of aluminum, arising from MST's close fitting, conducting, aluminum shell had never been measured.

We start by applying the multifoil spectrometer to a typical high-current discharge, the parameters of which are displayed in Fig. 3. Focusing on the oxygen measurement, Fig. 4(a) shows the measured emission of the 18–19 and 20–23 Å bands. Although the 18 Å band consists of emission from both O III ($1s-2p$) and O VII ($1s^2-1s3p$), the ratio of O VII ($1s^2-1s3p$) to O VII ($1s^2-1s2p$) varies slowly with electron temperature, and since the 20 Å band results almost exclusively from O VII ($1s^2-1s2p$), the relative emission of each state can be decoupled [Fig. 4(b)]. Aided by the fact that the electron temperature and density profiles are very flat
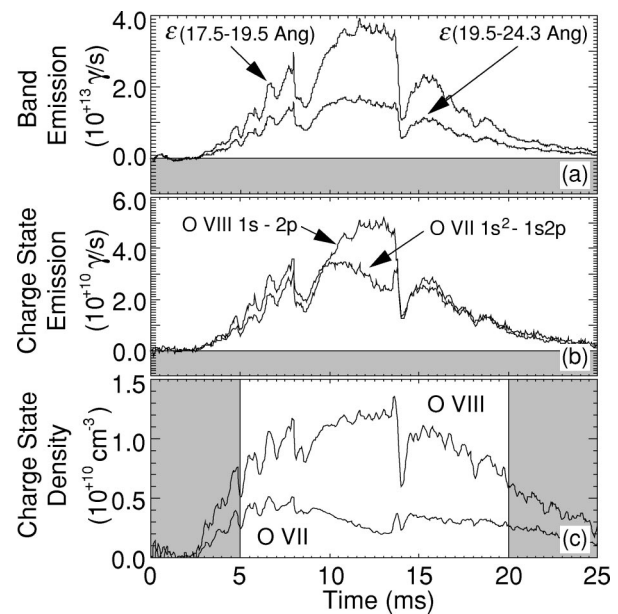

FIG. 4. Measured (a) emission from the 18–19 and 20–23 Å energy bands, (b) line intensities of the principal transitions of O VII and O VIII charge states, and (c) extracted O VII and O VIII charge-state densities.

over the plasma cross section, and assuming we have a Maxwellian temperature distribution, the excitation rates for these transitions can be calculated.[8] Once the excitation rates are known, we can estimate the chord-averaged densities of the O VII and O VIII charge states. Shown in Fig. 4(c), we see that at 10 ms, the density of O VIII begins to increase while O VII starts falling, indicating that O VII is burning through. This behavior continues until the sawtooth crash (magnetic relaxation event) cools the plasma and intensifies radial transport, thereby reducing the concentration of the highly ionized charge states.

The carbon information is more difficult to interpret. Unraveling the emissivity of the 25–35 and 37–43 Å channels, presented in Fig. 5, is complicated by both the nitrogen contamination of the 25–35 Å region and low photon intensity seen between 37 and 43 Å. Although we cannot specify with a high degree of certainty which impurities are responsible for the emission in the 25–35 Å region, the emission behavior does yield important information. Looking again at the time between 10 and 15 ms, the emission of C V is roughly constant, indicating that this charge state has already burned through and the profile is most likely very hollow. The decrease in emission between 25 and 35 Å indicates that, as in the case for O VII, the impurity responsible for this emission (be it carbon or nitrogen) is also burning through.
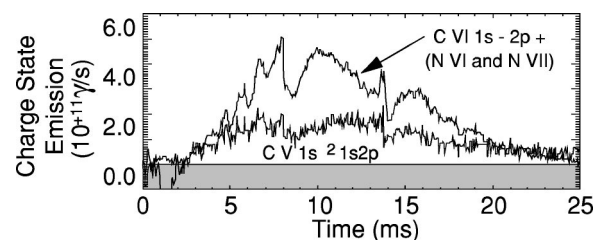

FIG. 5. Measured line intensities from C VI (with possible nitrogen contamination) and C V.
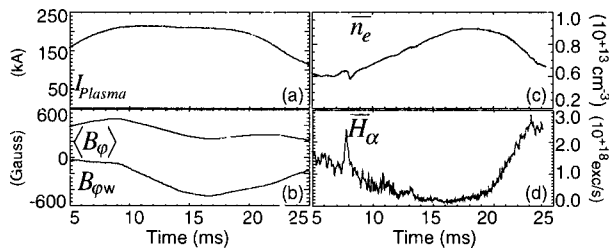
FIG. 6. (a) Plasma current, (b) average toroidal magnetic field and toroidal field measured at the wall, (c) line-averaged electron density measured through a central chord, and (d) the line-averaged H_α excitation rate for a high-confinement plasma discharge.

FIG. 7. Line intensity of the Al XII He-like 1.5 keV $1s^2-1s2p$ transition.

At high electron temperatures (> 500 eV), emission from Al XII becomes clearly visible. These temperatures are readily achieved during enhanced confinement auxiliary current drive experiments.[12,13] An ensemble of 137 shots was conducted and the parameters of these are illustrated in Fig. 6. Three aspects of these discharges are particularly relevant to Al XII emission. With electron density and temperature rising ($\sim 200–550$ eV), the number of high-energy electrons capable of ionizing to Al XII is increased. Most importantly, the neutral particle density drops, dramatically reducing the principal recombination mechanism for low-Z impurities. These effects couple to enhance the production and sustainment of high charge states.

An ensemble of the high-energy emission ($E>1$ keV) from these discharges, resulting from the $1s^2-1s2p$ transition of AL XII, is displayed in Fig. 7. The emission from AL XII is so bright that the lower-energy transitions (> 40 Å) dominate the boron and carbon channels of the spectrometer. A difficulty in the analysis of the Al XII is the lack of temporal behavior of the electron temperature. With further studies mapping the electron temperature in enhanced confinement discharges underway, the ability to transform Al XII emission to a charge-state density will soon be realized.

VI. CONCLUSIONS

We have developed a low-cost, robust, multilayer filtered spectrometer capable of obtaining absolute line intensity measurements of H- and He-like oxygen, carbon, and aluminum. Specifically, we observe that the redesigned multilayer coatings provide excellent isolation of the $1s-2p$
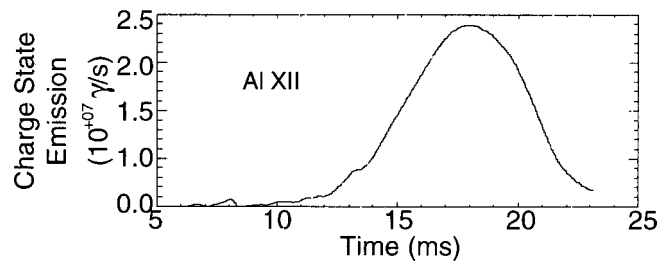
of O VIII and the $1s^2-1s2p$ of O VII and Al XII. In cases where nitrogen and aluminum contamination is known to be small, these transitions can also be resolved for C V and C VI. With the additional measurements of electron density and temperature, these absolute intensities can be used to extract the density of the emitting charge state. In the future, we hope to enhance the separation between carbon and nitrogen by implementing additional filters utilizing titanium and scandium.

ACKNOWLEDGMENTS

[1] P. A. Ross, J. Opt. Soc. Am. **16**, 433 (1928).
[2] P. Kirkpatrick, Rev. Sci. Instrum. **10**, 186 (1939).
[3] P. Kirkpatrick, Rev. Sci. Instrum. **15**, 223 (1944).
[4] H. A. B. Bodin and A. A. Newton, Nucl. Fusion **19**, 1255 (1980).
[5] S. Hokin, R. Fonck, and P. Martin, Rev. Sci. Instrum. **63**, 5038 (1992).
[6] L. Marrelli, P. Martin, and A. Murari, Meas. Sci. Technol. **6**, 1690 (1995).
[7] R. N. Dexter, D. W. Kerst, T. W. Lovell, S. C. Prager, and J. C. Sprott, Fusion Technol. **19**, 131 (1991).
[8] R. Mewe, Astron. Astrophys. **20**, 215 (1972).
[9] Oxford Research Corp., Richmond, CA.
[10] J. Seely, R. Korde, F. Hanser, J. Wise, G. E. Holland, J. Weaver, and J. C. Rife, Characterization of Silicon Photodiode Detectors with Multilayer Filter Coatings for 17–150 Angstroms, SPIE Meeting, 18–23 July 1999 (unpublished).
[11] International Radiation Detectors, Torrance, CA.
[12] J. S. Sarff, S. A. Hokin, H. Ji, S. C. Prager, and C. R. Sovinec, Phys. Rev. Lett. **72**, 3670 (1994).
[13] J. S. Sarff, N. E. Lanier, S. C. Prager, and M. R. Stoneking, Phys. Rev. Lett. **78**, 62 (1997).